ANTIMICROBIAL AGENTS AND CHEMOTHERAPY, Dec. 2004, p. 4532–4541 Vol. 48, No. 12
0066-4804/04/$08.00+0 DOI: 10.1128/AAC.48.12.4532–4541.2004

PnuC and the Utilization of the Nicotinamide Riboside Analog 3-Aminopyridine in *Haemophilus influenzae*

Elizabeta Sauer,[1] Melisa Merdanovic,[1] Anne Price Mortimer,[2] Gerhard Bringmann,[2] and Joachim Reidl[1]*

Institut für Hygiene und Mikrobiologie[1] and Institut für Organische Chemie, Lehrstuhl für Organische Chemie I,[2] Universität Würzburg, Würzburg, Germany

Received 6 May 2004/Returned for modification 22 July 2004/Accepted 18 August 2004

The utilization pathway for the uptake of NAD and nicotinamide riboside was previously characterized for *Haemophilus influenzae*. We now report on the cellular location, topology, and substrate specificity of PnuC. *pnuC* of *H. influenzae* is only distantly related to *pnuC* of *Escherichia coli* and *Salmonella enterica* serovar Typhimurium. When *E. coli* PnuC was expressed in an *H. influenzae pnuC* mutant, it was able to take up only nicotinamide riboside and not nicotinamide mononucleotide. Therefore, we postulated that PnuC transporters in general possess specificity for nicotinamide riboside. Earlier studies showed that 3-aminopyridine derivatives (e.g., 3-aminopyridine adenine dinucleotide) are inhibitory for *H. influenzae* growth. By testing characterized strains with mutations in the NAD utilization pathway, we show that 3-aminopyridine riboside is inhibitory to *H. influenzae* and is taken up by the NAD-processing and nicotinamide riboside route. 3-Aminopyridine riboside is utilized effectively in a *pnuC*$^+$ background. In addition, we demonstrate that 3-aminopyridine adenine dinucleotide resynthesis is produced by NadR. 3-Aminopyridine riboside-resistant *H. influenzae* isolates were characterized, and mutations in *nadR* could be detected. We also tested other species of the family *Pasteurellaceae*, *Pasteurella multocida* and *Actinobacillus actinomycetemcomitans*, and found that 3-aminopyridine riboside does not act as a growth inhibitor; hence, 3-aminopyridine riboside represents an anti-infective agent with a very narrow host range.

Bacterial species of the family *Pasteurellaceae* are dependent on nicotinamide substrates in the growth media, and NAD is an essential growth factor (30, 36). Cultivation of *Haemophilus influenzae* relies on the presence of either nicotinamide riboside (NR), nicotinamide mononucleotide (NMN), or NAD(P) (6). Other members of the *Pasteurellaceae*, so-called NAD-independent species, such as *Haemophilus ducreyi*, *Actinobacillus* spp., and *Pasteurella* spp., are, in addition, able to scavenge nicotinamide (Nam) (31), which might be utilized by diffusion and which is available in common complex bacterial growth media. To convert Nam to NMN, an immediate precursor for the resynthesis of NAD, the enzyme activity of NadV, a nicotinamide phosphoribosyltransferase, is required (27, 43, 44) (Fig. 1).

Prior to the successful introduction of the *H. influenzae* type b conjugate vaccine, *H. influenzae* type b infections were the main cause of bacterial meningitis (42). *H. influenzae* is still a major cause of otitis media and pneumonia. Therefore, studies were undertaken with the aim of exploring new therapeutics for *H. influenzae*. As reported earlier, 3-aminopyridine adenine dinucleotide (3-AAD) (Fig. 1B) inhibits *H. influenzae* growth. In those studies 3-AAD or the mononucleotide form (3-AMN) acted only as weak competitors for NAD utilization (5, 11, 17). The origin of growth inhibition could not be identified, and it was suggested that it interferes with the NAD(P)-dependent oxidoreductase, fermentation, and alternative respiration. However, it has also been demonstrated that 3-AAD acts as an effective inhibitor of NAD-dependent dehydrogenases (8). For *H. influenzae* NADP-dependent enzymes such as malate and 6-phosphogluconate dehydrogenases are also inhibited effectively by 3-aminopyridine analogs in vitro, but higher concentrations are needed compared with those required for growth inhibition (48, 49).

Recently, we have unraveled the NAD uptake pathway in *H. influenzae* and have identified membrane and periplasmic protein components such as porins, enzymes, and transporters necessary for NAD, NMN, and NR utilization The present model is depicted in Fig. 1A, in which OmpP2 represents a porin with specificity toward NMN and NAD; *e*(P4) is a lipoprotein encoded by the gene *hel* (12) that encodes a nucleotide phosphatase necessary to hydrolyze NMN to NR; NadN was described as a nucleotidase located in the periplasm that is needed to hydrolyze NAD to AMP and NMN and that with lower levels of activity is able to dephosphorylate NMN to NR; and finally, PnuC was identified as a permease acting in NR uptake (1, 15, 19, 33, 35). In other recent studies it was shown that *nadR* encodes an NR kinase and adenylytransferase and is able to resynthesize NAD from NR and NMN (20, 37). In the study described in this report, we have further characterized the transporter PnuC, the growth inhibition produced by 3-aminopyridine riboside (3-AmPR) derivatives (Fig. 1B), the routes of uptake of 3-AmPR derivatives, and the effects of 3-AmPR derivatives on the NAD resynthesis pathway.

* Corresponding author. Mailing address: Institut für Hygiene und Mikrobiologie, Universität Würzburg, Josef-Schneider-Str. 2, Bau 17, 97080 Würzburg, Germany. Phone: 49 931 20146159. Fax: 49 931 20146445. E-mail: joachim.reidl@mail.uni-wuerzburg.de.

MATERIALS AND METHODS

Bacterial strains and growth media. All strains used in this study are listed in Table 1. Strain *H. influenzae* Rd KW20 was originally obtained from A. Wright (Tufts University Boston, Mass.). In general, *H. influenzae* strains were cultured

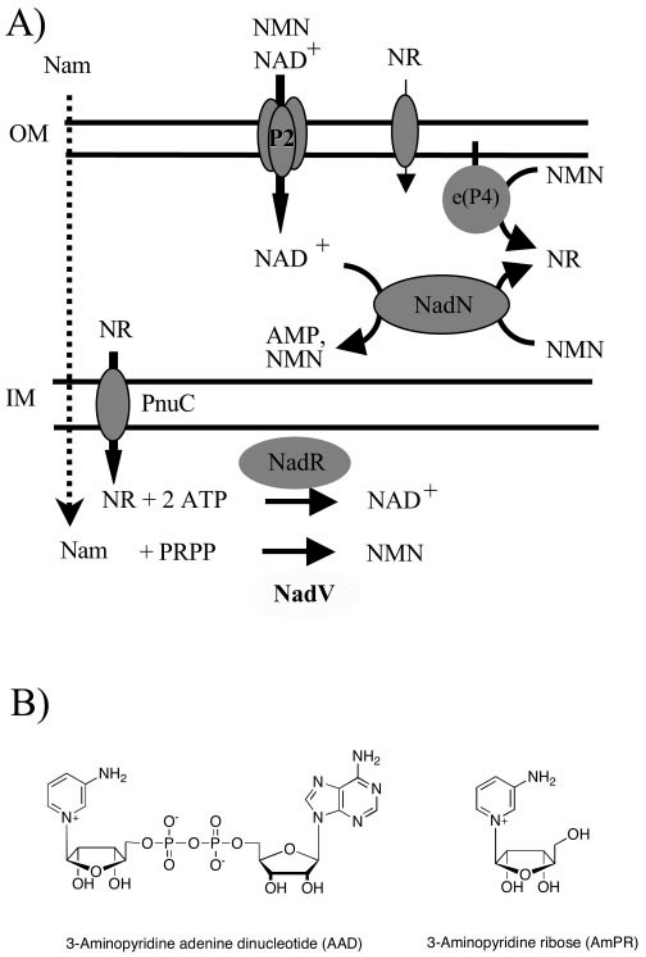

FIG. 1. NAD utilization model and inhibitor substrates. (A) Present model of NR, NMN, and NAD utilization pathway in *H. influenzae*. See text for more explanations. In extension to other isolates of the family *Pasteurellaceae*, the *nadV* gene, which encodes a nicotinamide phosphoribosyltransferase, is indicated in the transparency mode, which allows *H. influenzae* to utilize Nam as well. OM and IM, outer and inner membranes, respectively; PRPP, phosphoribosyl pyrophosphate. (B) Structure of the inhibitors 3-AAD and 3-AmPR.

in brain heart infusion (BHI) broth (Novagen/Merck, Darmstadt, Germany) or BHI agar supplemented with NAD or NR (15 μM each) and hemin (10 μg/ml). For *H. influenzae* cultures antibiotics were supplemented as described by Barcak et al. (2). *E. coli* strains were cultured in Luria-Bertani (LB) broth or on LB agar plates, supplemented when necessary with kanamycin (50 μg/ml), tetracycline (12 μg/ml) chloramphenicol (30 μg/ml), or ampicillin (100 μg/ml).

DNA purification, PCR, and DNA sequencing. Isolation and preparation of chromosomal DNA were done by the method of Grimberg et al. (13). PCRs for sequencing and subcloning were carried out with the TripleMaster system (Eppendorf, Hamburg, Germany). DNA sequencing was performed with an ABI 310 genetic analyzer (Applied Biosystems, Weiterstadt, Germany).

Construction of an *nadV*$^+$ *H. influenzae* strain. The intention to construct an *nadV*$^+$ *H. influenzae* strain was to relieve *H. influenzae* from NR-dependent growth and to enable genetic manipulation of the NR uptake pathway (Fig. 1A). The *H. ducreyi nadV* gene was characterized before (27, 45). We obtained *H. ducreyi* strain ATCC 27722 from the American Type Culture Collection. DNA was prepared from this strain, and *nadV* was amplified by PCR with oligonucleotides nadV5′EcoRV and nadV3′EcoRV (Table 2). A 2,000-bp fragment was obtained and subcloned into plasmid pSEhel, which was opened by digestion with SwaI (33). The SwaI sequence is located 7 bp downstream of the stop codon of the *hel* gene. The ligation resulted in plasmid pSEnadV. We amplified a 3,950-bp DNA fragment by PCR with pSEnadV as the template and oligonucleotides hel5′PstI and hel3′EcoRV (Table 2). This DNA fragment contains the intact *hel* gene, followed by *nadV* and the remaining 700-bp sequence of the *hel* downstream region. Subsequently, this DNA fragment was transformed into *H. influenzae* strain AK01 (14), and transformants were plated onto BHI agar plates supplemented with hemin but with no source of NAD. Growing colonies were obtained, and *nadV* integration into the chromosome was verified by PCR and Southern blot analysis. This construction yielded a *H. influenzae nadV*$^+$ strain which was able to grow independently of external NAD sources. The resulting AK01 *nadV*$^+$ strain was named SE01 (Table 1).

***pnuC* deletion mutant construction.** A DNA fragment was constructed to generate a complete deletion of the *pnuC*-encoding gene. The fragment consisted of 202 bp of a nonencoding fragment of the 5′ upstream region of *pnuC* (coordinates 1145266 to 1145064), followed by a kanamycin resistance gene cassette (*kanR*) and 277 bp of a nonencoding fragment of *pnuC* (coordinates 1144367 to 1144090) located in the 3′ downstream region. The 5′ region was generated with oligonucleotides PnuC1 and PnuC2 (Table 2). The 3′ region was generated with oligonucleotides I6 and PnuC4 (Table 2). We used chromosomal DNA prepared from strain AK01 to generate the respective PCR fragments. The *kanR* gene fragment (1,600 bp) was generated by digesting plasmid pUC4k (40) with PstI and StuI. Next, the two PCR fragments flanking *pnuC* (see above) and *kanR* were ligated together. Subsequently, the ligation mixture was used as a template in a PCR with oligonucleotides PnuC1 and PnuC4. This resulted in an amplified *kanR* fragment (2,079 bp) that contained the flanking *pnuC* upstream and downstream regions and the *kanR* promoter and termination sequences. This PCR product was subsequently transformed into *H. influenzae* strain SE01 (*nadV*$^+$) and AK01. After transformation, cells were plated onto BHI agar plates supplemented with kanamycin (10 μg/ml), and kanamycin-resistant colonies were isolated. After colony purification, chromosomal DNA was prepared, and PCR analysis with oligonucleotides PnuC1 and PnuC4 showed that the *kanR* gene was recombined into the chromosome and had replaced the *pnuC*-encoding reading frame (data not shown). This manipulation resulted in strains SE02 (*nadV*$^+$ Δ*pnuC*) and SE03 (Δ*pnuC*) (Table 1).

Genetic determination of PnuC topology. We performed protein fusion constructions of *pnuC* with *phoA* and *lacZ* genes. The locations of the insertions have been chosen according to a computerized transmembrane topology model of PnuC. To establish a topology model we used various programs: the TMPRED server, available at http://bioweb.pasteur.fr/seqanal/protein/; the PRED-TMR server, available at http://biophysics.biol.uoa.gr/cgi-bin/PRED-TMR/PRED-TMR; the DAS server, available at http://www.sbc.su.se/~miklos/DAS/maindas.html; the TMHMM server, available at http://www.cbs.dtu.dk/services/TMHMM/ (38); and the SOSUI server, available at http://sosui.proteome.bio.tuat.ac.jp/welcomeE.html. We used plasmid pSWFII (kindly provided by M. Ehrmann) as a donor for the *phoA* gene. pSWFII was digested with EcoRV and SmaI to obtain a 1,430-bp *phoA* sequence with no encoding signal sequence. The *lacZ* gene was obtained from *E. coli* strain C600. The gene fragment was amplified by using the oligonucleotides 5′-lacZ and 3′-lacZ (Table 2); the amplified fragment includes the stop codon but not the ribosome binding site or the initiation start codon. Plasmid pSEpnuC (15) was used as a template for PCR amplification of the whole plasmid to introduce StuI restriction sites into *pnuC*, which were used to generate *phoA* (in which a blunt end was generated with the EcoRV and SmaI fragments) or *lacZ* fusions (in which a blunt end was generated with SmaI). The oligonucleotides used for the amplification of plasmids with flanking StuI restriction sites are listed in Table 2. After PCR amplification the products were religated and transformed into *E. coli* strain BL21 (Novagen/Merck, Darmstadt, Germany) and plated onto LB agar with chloramphenicol (30 μg/ml). Single colonies were picked, and plasmid DNA was prepared as described above. Isolated pSEpnuC(StuI) plasmids were cut with StuI, dephosphorylated with shrimp alkaline phosphatase (Amersham Bioscience, Freiburg, Germany), and ligated with fragments of either the *phoA* or the *lacZ* gene added to the mixture. Each of these ligated fragments was then transformed into *E. coli* strain CC118 (26). Transformants were plated onto LB agar with chloramphenicol (30 μg/ml) supplemented either with the substrate 5-bromo-4-chloro-3-indolyl-β-D-galactopyranoside (X-Gal; 40 μg/ml) for the β-galactosidase (LacZ) or with 5-bromo-4-chloro-3-indolylphosphate (XP; 40 μg/ml) for the alkaline phosphatase (PhoA). Colonies active in the presence of X-Gal and XP and also single white colonies were isolated and purified. Subsequently, plasmid DNA was prepared and analyzed for *phoA* or *lacZ* fragment insertion by restriction analysis. Finally, the junctions between *phoA*, *lacZ*, and *pnuC* were verified by DNA sequencing (data not shown).

Cloning of *E. coli pnuC* and expression in *H. influenzae*. The *pnuC* gene of *E. coli* strain C600 (New England Biolabs, Inc., Frankfurt, Germany) was subcloned. Specific oligonucleotides were used to generate a DNA fragment encoding the *pnuC* gene. The oligonucleotide E.copnuC5′ was used for the 5′ end, and oligonucleotide E.copnuC3′ was used for the 3′ end (Table 2). The 827-bp *pnuC* DNA fragment generated was cut with restriction enzymes EcoRV and BamHI

TABLE 1. Relevant strains and plasmids used in this study

Strain or plasmid	Relevant phenotype or genotype	Reference or source
Strains		
H. ducreyi	*nadV*$^+$, ATCC 27722	4
H. influenzae Rd KW20	Genome sequence determined	9
AK01	Strain Rd (*sxy*-1 Str^r) constitutive competent	14
SE01	AK01 expressing *nadV*$^+$ on chromosome	This study
SE02	SE01, Δ*pnuC*::*kan* Kan^r	This study
SE03	AK01, Δ*pnuC*::kan Kan^r	This study
REI1010	Strain Rd (*nadN*::*cat*) Cm^r	33
REI1012	Strain Rd (Δ*hel*::*kan*) deficient for *e*(P4), Kan^r	19
GK04	Strain Rd (*nadN*::*cat* Δ*hel*::*kan*) Cm^r Kan^r	19
H. influenzae Δ*ompP2*	Strain Rd (Δ*ompP2*::*cat*) cm^r	1
P. multocida A3	Serogroup A3	L. Weiler
A. actinomycetemcomitans CU4000N		7
Plasmids		
pACYC184	Cm^r Tet^r	New England Biolabs
pSEhel	Cm^r	33
pSEnadV	Cm^r	This study
pSEpnuC	Cm^r	15
pSEpnuC$_{E.\ coli}$	Cm^r	This study
pSEpnuC-His$_6$N′/C′	Tet^r	This study
pMMnadR-His$_6$	Amp^r	This study

and ligated to plasmid pACYC184, which was opened by digestion with EcoRV and BamHI (34). Subsequently, the ligation mixture was transformed into *E. coli* strain LE392 (New England Biolabs) (23) and plated onto LB agar supplemented with chloramphenicol (30 μg/ml). Colonies were isolated, plasmid DNA was prepared, and PCR analysis was performed to identify the cloned *E. coli* *pnuC* fragment. Verification that the fragment had been inserted was done by restriction digestion (data not shown). Subsequently, *pnuC*-positive clones were transformed into *H. influenzae* strain SE02 (*nadV*$^+$ Δ*pnuC*) and *H. influenzae* strain REI1012 (Δ*hel*). REI1012 was previously constructed as a mutant from which the complete *hel* gene, which encodes the outer membrane lipoprotein *e*(P4), was deleted and in which a kanamycin resistance-conferring gene, *kanR*, replaced *hel* (19).

Construction of His-tagged PnuC and NadR expression systems. Plasmid pSEpnuC was used to construct N′- and C′-terminal His-tagged PnuC hybrid proteins, while chromosomal DNA of strain AK01 was used to construct the C′-terminal His-tagged NadR chromosomal DNA. For construction of the His-tag at the C′ terminus, PCR amplification was undertaken with oligonucleotides pnuC5′CHis and pnuC3′CHis for *pnuC* and oligonucleotides nadRItopo5′ and nadRItopo3′ for *nadR* (Table 2). Purified *pnuC*- and *nadR*-encoding DNA fragments were cloned into the pCRT7-CT-TOPO vector (Invitrogen, Karlsruhe, Germany) according to the directions in the manufacturer's manual, thus creating *pnuC* and *nadR* fragments carrying the V5 epitope and a six-His tag at their C′ termini. The ligation mixture was transformed into TOP10F′ *E. coli* cells and plated onto LB agar with ampicillin (100 μg/ml), and Amp^r colonies were selected. Plasmids pCRT7-TOPOpnuCHis$_6$ and pMMNadR-His$_6$ were obtained. Plasmids were prepared from isolated colonies; and the constructs were verified by restriction analysis, DNA sequencing, sodium dodecyl sulfate-polyacrylamide gel electrophoresis (SDS-PAGE), and Western blot analysis with anti-His antiserum (Qiagen, Hilden, Germany) for poly-His domains by standard methods (21, 41) (data not shown).

For the construction of PnuC with a His tag at the N′ terminus, PCR was performed with plasmid pSEpnuC and oligonucleotides PnuC5′pIVEXHis and PnuC3′pIVEXHis (Table 2). For subcloning of the poly-His sequence, the PCR fragment was ligated into plasmid pIVEX2.4b (Roche Molecular Biochemicals, Mannheim, Germany), which was opened by digestion with XhoI and PstI. After ligation, transformation, and plating, Amp^r colonies were purified and the plasmids yielded by the colonies were prepared. The plasmid obtained was pIVEX-pnuCHis$_6$. We verified the constructs by restriction analysis, PCR analysis, and DNA sequencing (data not shown). In addition, the transformed *E. coli* clones were tested by SDS-PAGE and Western blot analysis by standard methods (21, 41) by using anti-His antiserum (Qiagen) for poly-His domains.

To express the C′- and N′-terminal PnuC hybrid proteins in *H. influenzae*, each fusion protein construct was further subcloned into plasmid pACYC184. For subcloning of the fusion protein constructs, pCRT7-TOPOpnuCHis$_6$ and pIVEX pnuCHis$_6$ were used as the templates and oligonucleotides CT-Topo5′ and CT-Topo3′ and oligonucleotides pIVEX2.4b5′ and pIVEX2.4b3′, respectively (Table 2), were used. pACYC184 was digested with restriction enzymes EcoRI and ScaI; the respective PCR fragments were ligated; the samples were transformed into *E. coli* (LE392) and plated onto LB agar with tetracycline (12 μg/ml); Tet^r colonies were isolated; and the plasmids were tested by PCR, restriction analysis, and DNA sequence analysis (data not shown). Finally, the resulting plasmids were termed pSEpnuC-His$_6$ (C′- and N′-terminal constructs). Subsequently, the plasmids were transformed into *H. influenzae* SE02, and cell extracts were analyzed by SDS-PAGE and Western blotting, which demonstrated that His-tagged PnuC hybrid proteins were produced (see Fig. 3).

His-tagged NadR protein purification. His-tagged NadR protein was expressed in *E. coli* BL21(DE3)(pLysS) as a C′-terminal V5-His$_6$ tag fusion protein. Cultures (400 ml) were grown in LB medium with ampicillin at 37°C with shaking to an optical density at 600 nm (OD_{600}) of 0.8. The temperature was adjusted to 18°C, and expression was induced with isopropyl-β-D-thiogalactopyranoside (0.8 mM). Cells were harvested after 18 h of shaking at 18°C. For protein purification, cells harvested from 400 ml of culture were washed and resuspended in 4 ml of NaH_2PO_4 (50 mM)–NaCl (300 mM) (pH 8) containing mercaptoethanol (2 mM), Brij 35 (0.03%), and a protease inhibitor mixture (complete, EDTA-free; Boehringer Ingelheim, Ingelheim, Germany). The cells were lysed in a French press, and the lysate was centrifuged to remove the cell debris (7,700 × *g*, 4°C, 20 min). The supernatant was loaded onto a Protino 1000 column that had been equilibrated with the same buffer. The column was washed with starting buffer containing Brij 35 (0.3%), and afterwards, the bound proteins were eluted with starting buffer containing imidazole (250 mM). The eluted fractions were analyzed by SDS-PAGE. Protein samples were shock frozen with liquid nitrogen, and aliquots were stored at −80°C.

PhoA and LacZ activities. To determine the enzyme activity of *pnuC-phoA* and *pnuC-lacZ* fusions, the alkaline phosphatase and β-galactosidase assays were performed by the methods described earlier (24, 29). The activities were expressed in Miller units of absorption, expressed as $\Delta OD_{405}/(OD_{600}\ 1 \times 1$ milliliter × 1 minute).

Cell fractionation and cell extracts. *H. influenzae* SE02 was transformed with C′- and N′-terminal versions of pSEpnuC-His$_6$ and control plasmid pACYC184. Transformants were then used to prepare cellular and membrane extracts. Strains were grown in 25 ml of BHI medium (see above) to an OD_{490} of 2. After centrifugation at 3,000 × *g* for 5 min, the pellets were resuspended in 100 μl of HEPES (50 mM; pH 7.5) containing protease inhibitor (Roche Diagnostics, Mannheim, Germany). Cells were opened by shearing the cells with glass beads in a cell shredder (Bio 101, Savant Instruments Inc., New York, N.Y.). To remove whole cells, the lysates were centrifuged at 3,000 × *g* at 4°C for 5 min. The cell extracts were centrifuged in an ultracentrifuge (Optima TL; Beckman Coulter, Krefeld, Germany) at 300,000 × *g* for 20 min. The supernatants were

TABLE 2. Oligonucleotides used for plasmid and strain constructions

Oligonucleotide name	Sequence[a]
nadV5′EcoRV	5′-TAGATATCAGACTTATGTCTCGGAGTATAACG-3′
nadV3′EcoRV	5′-TTGATATCTCATAGCGTAGTGCGACTAAC-3′
hel5′PstI	5′-AAAACTGCAGCAGAAAGACTTACTATACCCTG-3′
hel3′EcoRV	5′-TCGATATCACAAATGCGCTATTCTGACGGG-3′
PnuC1	5′-CGACGTTCGTCAATGGTCTT-3′
PnuC2	5′-AACTGCAGGAGGTGACCATTTTCGCATTG-3′
I6	5′-AAAGGCCTGCGTACTAACTAAATATAAAAACAG-3′
PnuC4	5′-CCTTGGTTTGTCGCTTGTCA-3′
5′-lacZ	5′-TTCCCGGGTTATGATTACGGATTCACTGGCCGTC-3′
3′-lacZ	5′-TTCCCGGGATAGTACATAATGGATTTCCTTACGCG-3′
E.copnuC5′	5′-TTTGATATCTTGCGGCTACACTACGTGGA-3′
E.copnuC3′	5′-AAAGGATCCAGACTGCCACCTGAATGAAG-3′
pnuC5′CHis	5′-ATGACTTTGGCAGCGCGTTTA-3′
pnuC3′CHis	5′-GTTAGTACGCTTAACTAACTAATTTCGTCCAGTT-3′
nadRItopo5′	5′-GTGGGCTTTACCACCGGTAGGGAAT-3′
nadRItopo3′	5′-TTGAGATGTCCCTTTTATAGGAAAG-3′
PnuC5′pIVEXHis	5′-TTACTCGAGACTTTGGCAGCGCGTTTAAAACA-3′
PnuC3′pIVEXHis	5′-ATTCTGCAGTTATATTTAGTTAGTACGCTTAAC-3′
CT-Topo5′	5′-AAAGAATTCAGACCACAACGGTTTCCCTCTA-3′
CT-Topo3′	5′-TTTAGTACTTGCTCAGCTAAGGTTTCTTCT-3′
pIVEX2.4b5′	5′-AAAGAATTCGAGACCACAACGGTTTCCCTCTA-3′
pIVEX2.4b3′	5′-TTTAGTACTTTCCTTTCGGGCTTTGTTAGCA-3′
aa D39 3′	5′-AAAGGCCTGAGGTGTTTGTACATAAGCCCAAAT-3′
aa D39 5′	5′-AAAGGCCTGGTTAGCAATGATTTCTGGTATTTC-3′
aa V94 3′	5′-AAAGGCCTGGTAAAGTACGGTGTTCATTTCGCC-3′
aa V94 5′	5′-GGAGGCCTAATTTATTGGTTACTTTATGTGGAA-3′
aa S118 3′	5′-TTAGGCCTGTTCTCCACCATCGCTATTTTGCAT-3′
aa S118 5′	5′-AAAGGCCTGCGTGATTGCAAAAGCGTTAACTGT-3′
aa Q179 3′	5′-TTAGGCCTGTTCACGATAACGCAAAATCATTA-3′
aa Q179 5′	5′-TTAGGCCTTGGTTGTTATGGATTGGATTAAATA-3′
aa E196 3′	5′-AAAGGCCTGTCCCCATAAGAAAATAGAAAGAAT-3′
aa A150 3′	5′-AAAGGCCTGCGCTTGTAATGCTTGAACAAAA-3′
aa A150 5′	5′-AAAGGCCTGCTGGTGGTAGCTCAACAGGTTT-3′
aa E10 3′	5′-TTAGGCCTGTTGTTTTAAACGCGCTGCCAAAGT-3′
aa S63 3′	5′-TTAGGCCTGAATTTTACCTTTACTTACCAATAC-3′
aa S63 5′	5′-AAAGGCCTGCCTATACTTATTTTTATGTTGCT-3′
aa K220 3′	5′-AAAGGCCTGCGTCCAGTTATAATAACCATACAA-3′
aa K220 5′	5′-AAAGGCCTGCGTACTAACTAAATATAAAAACAG-3′

[a] Restriction sites are underlined.

stored overnight (ON) at 4°C, while the pellets were resuspended in 40 μl of HEPES (50 mM; pH 7.5) supplemented with Triton X-100 (2%) and agitated ON at 4°C. Subsequently, the samples were diluted 1:3 in HEPES (50 mM; pH 7.5) and incubated for 1 h at 37°C prior to SDS-PAGE analysis.

Nicotinamide nucleotide reagents and 3-aminopyridine derivatives. [Carbonyl-^{14}C]NAD was obtained from Amersham Bioscience, and [^{14}C]NMN was prepared from [carbonyl-^{14}C]NAD as described before (19). 3-Aminopyridine adenine dinucleotide phosphate (3-AADP) was purchased from Sigma Aldrich (Taufkirchen, Germany), and 3-AAD was synthesized as described before (8) and further processed to the 3-AmPR analog as described previously for the generation of NR from NAD (19). The reaction products were verified by thin-layer chromatography (TLC) (see below) and monitoring with UV light. 3-AAD was furthermore characterized by ^{1}H nuclear magnetic resonance spectroscopy with the inclusion of correlation spectroscopy (400 MHz; measured on a Bruker AMX-400 instrument with D_2O as the solvent and HOD [δ 4.70] as the internal standard [data not shown]).

TLC analysis. Reaction samples were separated by TLC in a solvent system consisting of 1 M ammonium acetate (pH 5) and ethanol (40:60) (18) on Cellulose F plates (Merck). By using radioactively labeled samples, after separation, the plates were dried and exposed to radiation-sensitive film (Eastman Kodak Co., Rochester, N.Y.). Spots were identified by comparison with reference samples of ^{14}C-labeled NAD, NMN, NR, and Nam.

[Carbonyl-^{14}C]NAD uptake studies. NAD uptake studies were performed with *H. influenzae* strains SE01, SE02(pSEpnuC$_{E.\ coli}$) and REI1012(pSEpnuC$_{E.\ coli}$). Uptake analysis was done as described before (19).

Determination of 3-AAD synthesis with purified NadR. Purified His-tagged NadR was used to demonstrate the synthesis of 3-AAD. The reaction mixture consisted of 3-AmPR (0.8 mM), ATP (5 mM), and $MgCl_2$ (10 mM) in HEPES (100 mM; pH 7.5) to which His-tagged NadR protein (50 μg/ml) was added. The reaction was carried out at 37°C ON. Subsequently, the reaction mixture was inactivated by heating at 100°C for 5 min and centrifugation (16,000 × *g*, 5 min), and the supernatant was subjected to high-pressure liquid chromatography (HPLC) analysis. HPLC was carried out on a Symmetry C_{18} column (4.6 by 250 mm; 5 μm; Waters) at a flow rate of 1 ml/min with isocratic elution with sodium dihydrogen phosphate (50 mM; pH 5.5) containing tetrabutylammonium bromide (8 mM) and methanol (8%); UV detection from 200 to 500 nm was carried out with a photodiode array detector, with monitoring at 254 nm. The reaction mixture was monitored for the presence of the 3-AmPR substrate and the 3-AAD product, whose identities were confirmed by analysis of the UV spectra of their peaks (data not shown).

3-AmPR and 3-AAD inhibition of NAD biosynthesis. An in vitro assay was established to investigate whether the presence of 3-AmPR or 3-AAD interferes with NAD synthesis by NadR. The reaction mixture consisted of [^{14}C]NR or [^{14}C]NMN (40 μM) and ATP (2 mM) with 3-AmPR or 3-AAD (0.5 and 1 mM, respectively), $MgCl_2$ (10 mM), and His-tagged NadR (50 μg/ml). The reaction volume was 40 μl in HEPES-NaOH (100 mM; pH 7.5), and incubation was carried out for 40 min at 37°C. The reactions were stopped by incubation at 100°C for 10 min, and the denatured protein was removed by centrifugation. Subsequently, the supernatants (sample volume, 10 μl) were analyzed by TLC (see above).

Inhibitor analysis with 3-aminopyridine derivatives and isolation of resistant mutants. Inhibitor analyses were performed as described before (11). *H. influenzae* strains AK01, SE01 (*nadV*$^{+}$), SE02 (*nadV*$^{+}$ Δ*pnuC*), and SE03 (Δ*pnuC*) were used in the experiments. In brief, incubation was done with substrate (NADP)/inhibitor (3-AADP) ratios of 1:50 and 1:100. Cells were diluted so that the samples contained 10^5 CFU and were inoculated into BHI growth medium

supplemented with hemin and with NADP and 3-AADP at various ratios. After 24 h, the cells were serially diluted onto BHI agar plates, and the numbers of viable cells were counted. In a second assay, growth analyses were performed with different *H. influenzae* NAD uptake mutants, *Pasteurella multocida* A3, and *Actinobacillus actinomycetemcomitans*. Growth was monitored after 24 h of incubation on BHI medium supplemented with hemin and NR (15 μM) and a 1:100 fold excess of 3-AmPR, 3-AAD, or 3-AADP compared to the amount of NR.

A growth selection method was established to isolate mutants that were able to grow in the presence of 3-AmPR. Selection was performed on BHI agar plates supplemented with 3-AmPR (65 μM). Then, strain SE01 (*nadV*$^+$) was plated and a few single growing colonies were observed. These were further isolated by growing them on BHI agar containing 3-AmPR. Subsequently, chromosomal DNA was generated from these isolates and used to amplify the *nadR* and *pnuC* gene fragments by PCR. The *pnuC*- and *nadR*-coding regions were then sequenced. Each clone was sequenced at least twice.

RESULTS AND DISCUSSION

PnuC specificity and location. In *H. influenzae* NR acts only as a substrate for the transporter PnuC, which is located on the inner membrane (15, 19). In *Salmonella enterica* serovar Typhimurium it was inferred that NMN could serve as a substrate for PnuC (39, 50, 51). The PnuC derived from *E. coli* shares about 89% identity at the amino acid level with the *S. enterica* serovar Typhimurium-encoded PnuC. To investigate whether the *E. coli*-derived PnuC would be able to transport NMN in *H. influenzae*, we subcloned *pnuC* of *E. coli* strain C600 carrying plasmid pSEpnuC$_{E.\ coli}$ and expressed it in *H. influenzae* strain SE02 (Δ*pnuC nadV*$^+$) and REI1012 (Δ*hel*) (19). With REI1012 (Δ*hel*), which is unable to utilize NMN (19), no uptake of NMN was observed (Fig. 2A), even if the cells were transformed with plasmid pSEpnuC$_{E.\ coli}$. However, in SE02(pSEpnuC$_{E.\ coli}$) NR uptake occurred at levels comparable to those in wild-type *H. influenzae* (Fig. 2B). This indicates that NR and not NMN serves as the substrate for PnuC derived from *E. coli* and most likely also serves as the substrate for the PnuC of *S. enterica* serovar Typhimurium. Therefore, NMN must be dephosphorylated to NR prior to uptake. Considering the distant relationship of the paralogous PnuC proteins of *H. influenzae* and *E. coli*, we claim that in general PnuC proteins most likely act as NR transporters. Early characterization of NMN uptake in *S. enterica* serovar Typhimurium via PnuC probably did not consider the phosphatase activities contained in the periplasm and prepared NR was never used as the substrate.

To show the cellular location of functional PnuC protein in *H. influenzae*, His-tagged constructs of the N′ and C′ termini were expressed by plasmids pSEpnuC-His$_6$N′ and pSEpnuC-His$_6$C′ in *H. influenzae*. The SE02 (*nadV*$^+$ Δ*pnuC*) mutant transformed with His-tagged PnuC-encoding plasmids took up [^{14}C]NR at a level similar to that for wild-type *H. influenzae* (data not shown). Subsequently, in cell fractionation, SDS-PAGE, and Western blot analyses, the His-tagged PnuC proteins were found to be associated with the cytosolic membrane fraction (Fig. 3, lanes 4 and 6).

PnuC topology. All integral membrane proteins have common basic architectural principles and cross the membrane in an alternating fashion, thereby exposing hydrophilic loops in the cytosolic and periplasmic compartments, while the hydrophobic α helices traverse the membrane (16). PnuC belongs to a class of abundant cytoplasmic integral membrane proteins that act as solute transporters. These proteins constitute ion

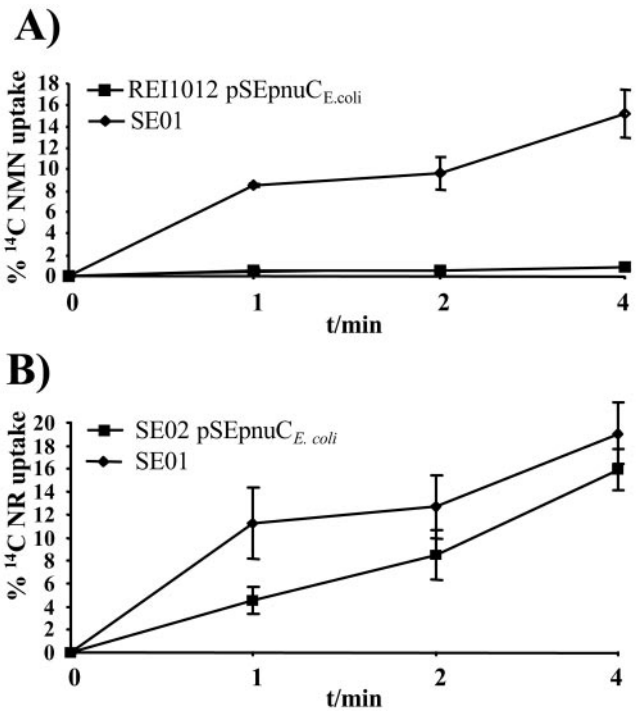

FIG. 2. [^{14}C]NR and [^{14}C]NMN uptake by PnuC derived from *E. coli* and expressed in *H. influenzae*. (A) Percent accumulation of ^{14}C-labeled material derived from [^{14}C]NMN by strains REI1012 (Δ*hel*) pSEpnuC$_{E.\ coli}$ and SE01 (*nadV*$^+$); (B) percent accumulation of ^{14}C-labeled material derived from [^{14}C]NR by strains SE02 (*nadV*$^+$ Δ*pnuC*) pSEpnuC$_{E.\ coli}$ and SE01. Experiments were performed at least in triplicate, and standard deviations are indicated. t/min, time (in minutes).

gradient-linked, ATP-driven, or group translocation systems (16). The topologies of many transmembrane proteins have been genetically resolved by using *phoA* and *lacZ* protein fusions (22, 25, 26). We also chose this approach and generated numerous protein fusions between PnuC and both PhoA and

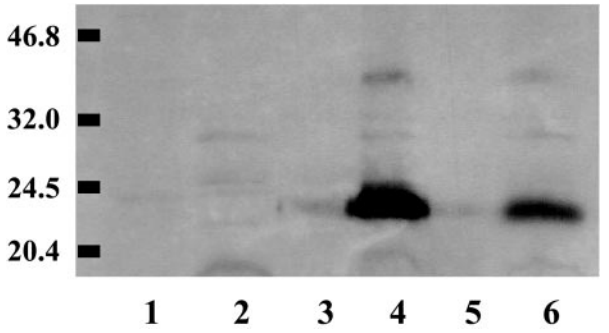

FIG. 3. PnuC localization in *H. influenzae* determined by Western blot analysis with PnuC proteins with His tags at the N′ and C′ termini. Lanes 1 and 2, controls consisting of cell extracts of SE02 (*nadV*$^+$ Δ*pnuC*)(pACYC184) supernatant (lane 1) and membrane pellet (lane 2); lanes 3 and 4, C′-terminal His-tagged PnuC constructs of the SE02(pSEpnuC-His$_6$C) supernatant (lane 3) and membrane pellet (lane 4); lanes 5 and 6, N′-terminal His-tagged PnuC constructs of the SE02(pSEpnuC-His$_6$N) supernatant (lane 5) and membrane pellet (lane 6). Numbers on the left are molecular sizes (in kilodaltons).

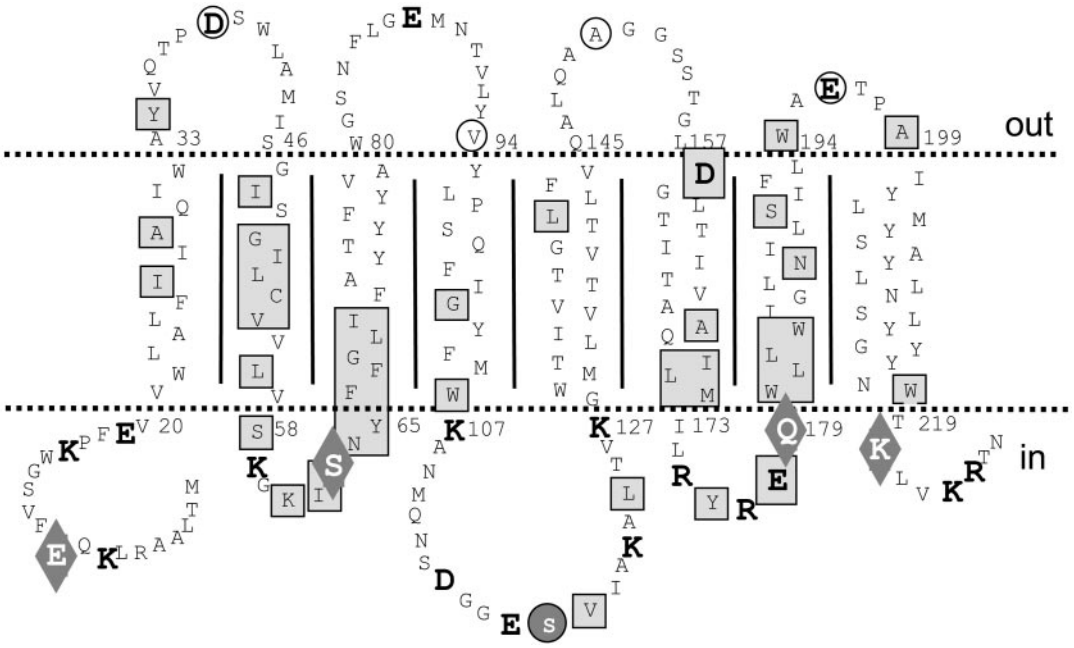

FIG. 4. Model of *H. influenzae* PnuC secondary structure. The model is based on several transmembrane prediction programs and the activities of the PnuC-PhoA and PnuC-LacZ fusions generated. White circles, positions of PnuC-PhoA fusions with high levels of activity; gray circles, positions of PnuC-LacZ fusions with high levels of activity; gray diamonds, positions of PnuC-LacZ and PnuC-PhoA fusions with high levels of LacZ activity but low levels of PhoA activity; shaded boxes, conserved amino acids in PnuC homologs of *Yersinia pestis*, *Enterococcus faecalis*, *Pseudomonas syringae*, *S. enterica* serovar Typhimurium, *Shigella flexneri*, *Vibrio cholerae*, and *E. coli*. Positively and negatively charged amino acids are superimposed onto the model.

LacZ (see Material and Methods). Only five to seven transmembrane helices were predicted on the basis of computerized transmembrane modeling in silico. We designed *phoA* and *lacZ* insertions to determine the secondary protein structures experimentally. The activities of alkaline phosphatase and β-galactosidase fused to the appropriate reading frame of PnuC were significant enough to ascribe the cellular location of each fusion junction. The calculated PhoA activities (in Miller units) for fusion point amino acid (aa) positions were as follows: for aa D39, 240; for aa V94, 80; for aa A150, 60; and for aa E196, 70. These were about 30- to 240-fold higher than those determined for PhoA fused to the predicted cytosolic domains at the fusion junction: for aa E10, 2; for aa S63, 1; for aa Q179, 1; and for aa K220, 2. The value was 1 Miller unit for the negative control. The PhoA activities of the PhoA fusion proteins in the periplasm differed fourfold (between 240 and 60 Miller units). A possible explanation, as indicated before (28), could be that the activities and levels of expression of PhoA fusions tend to decrease with fusion protein length and that long fusion proteins will be more unstable than shorter ones.

LacZ protein hybrid constructs in the cytoplasmic domains of PnuC produced significant β-galactosidase activities (in Miller units): for aa E10, 1,325; for aa S63, 200; for aa S118, 400; for aa Q179, 650; for aa K220, 450; and for the negative control, 2.5. No LacZ fusions could be generated with the periplasmic domains, as described for PhoA. For aa E10, aa S63, aa Q179, and aa K220 the LacZ activities that were determined and the lack of PhoA activities at the same insertion site confirm conclusively the expected locations of these domains. As a result, we can determine a topology model of the secondary protein structure when it is aligned to its transmembrane segments (Fig. 4). According to the resulting model, PnuC spans the membrane eight times, and both the N′ and the C′ termini are located on the cytosolic face.

Several PnuC-PhoA fusion constructs were tested by NAD uptake assays. We found that the disruption or truncation of the last transmembrane segment significantly reduced the transport activity. For example, as determined for strain SE01, 83% accumulation of [carbonyl-^{14}C]NAD was observed. The last *phoA* insertion at aa K220, which truncated only the last 7 amino acids, was significantly active in NAD utilization, with NAD accumulation of 52.5%. A PnuC-LacZ fusion at aa T179 resulted in 1.6% accumulation, and a fusion at aa A150 resulted in only 0.2% accumulation. Also, the absence of the last transmembrane domain, represented by the fusion at aa E196, allowed no uptake (<0.2%). These data indicate that only a limited truncation of PnuC is tolerated without interfering with its protein function. However, modification of the N′ and C′ termini seems to be tolerated, as we were able to generate His-tagged PnuC fusions at both ends of the protein, and after the fusions were expressed in SE02, they complemented NAD uptake to the same level as that for the wild-type strain (data not shown).

3-AmPR and growth deficiency in *H. influenzae*. As reported earlier, 3-AmPR derivatives inhibit *H. influenzae* growth (5, 11) but not *Staphylococcus aureus* or *E. coli* growth (11). Godek and Cynamon (11) showed that 3-AmPR inhibits growth if the molar ratio between NR and 3-AmPR is about 1:10. To resolve the route of entry, we adopted their assay using the compounds

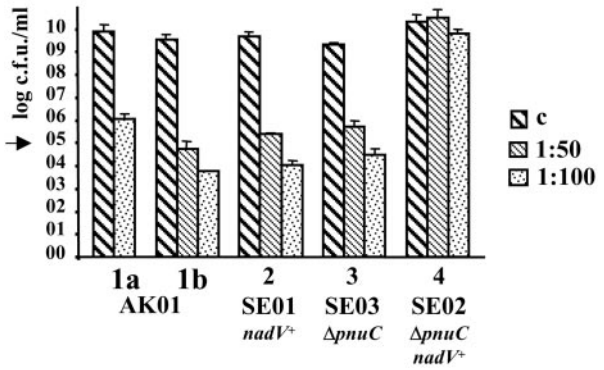

FIG. 5. 3-AADP growth inhibition study with different *H. influenzae* mutant strains. In the growth analysis (bars labeled 1b to 4) strains were grown under aerobic conditions (in BHI medium) in the presence of 3-AADP and NADP at molar ratios of 1:50 and 1:100. For the experiment, cells were diluted, inoculated at 10^5 CFU/ml (see arrow), and grown ON in the presence of 3-AADP. After 24 h the cells were plated and viable cells were counted (number of CFU per milliliter). Strain names and genotypes are provided at the bottom. Additionally, strain AK01 (lane 1a) was tested under anaerobic incubation conditions with a GasPak 150 incubator in a BBL GasPak generator with a catalyst (Baxter Diagnostics), but otherwise, the same procedure was applied to strain AK01 and the other strains tested.

3-AADP, 3-AAD, and 3-AmPR and investigated *H. influenzae* NAD uptake mutants, including *hel*, *ompP2*, *nadN*, *pnuC*, and *nadV*$^+$ strains. We assessed the viable cell count after 24 h of incubation of strains AK01, SE01 (*nadV*$^+$), SE02 (*nadV*$^+$ Δ*pnuC*), and SE03 (Δ*pnuC*) with commercially obtained 3-AADP (Fig. 5). We found that for wild-type strain AK01, the inhibitory action of 3-AADP was similar to that of 3-AAD observed by Godek and Cynamon (11). The inhibitory effect was also observed under anaerobic growth conditions (Fig. 5, bars 1a). For the other mutants (listed in Table 3) we monitored the growth in BHI supplemented with NR and aminopyridine derivatives 3-AADP, 3-AAD, and 3-AmPR.

Analysis of the growth of the mutant strains revealed the following pattern (Fig. 5): strains AK01 (Fig. 5, bars 1b), SE01 (*nadV*$^+$) (Fig. 5, bars 2), and SE03 (Δ*pnuC*) (Fig. 5, bars 3) were sensitive to 3-AADP, whereas strain SE02 (*nadV*$^+$ Δ*pnuC*) (Fig. 5, bars 4) was resistant. These differences (Fig. 5) suggest that PnuC is an effective entry gate for the 3-AmPR substrate. The result obtained with strain SE03 suggests that if PnuC is missing, then a second NR uptake route (as yet undefined) (15) remains active and permits 3-AmPR to be taken up. However, with a 1:100 excess of 3-AADP in an *nadV*$^+$ and Δ*pnuC* background, the second uptake route does not seem to be effective enough to compete with the function of NadV, which synthesizes NMN derived from Nam and therefore bypasses the inhibitor entry route.

TABLE 3. Growth ability on aminopyridine derivatives

Strain	Growth on[a]:			
	NR	3-AmPR	3-AAD	3-AADP
H. influenzae SE01 (*nadV*$^+$)	+	−	−	−
H. influenzae SE02 (*nadV*$^+$ Δ*pnuC*::*kan*)	+	+	+	+
H. influenzae SE02 (*nadV*$^+$ Δ*pnuC*::*kan*) (pSEpnuC-His$_6$C)	+	−	−	−
H. influenzae REI1012 (Δ*hel*)	+	−	+	+
H. influenzae REI1010 (*nadN*::*cat*)	+	−	+	+
H. influenzae GK04 (Δ*hel nadN*::*cat*)	+	−	+	+
H. influenzae (Δ*ompP2*::*cat*)	+	−	+	+
P. multocida A3	+	+	+	+
A. actinomycetemcomitans CU4000N	+	+	+	+

[a] NR was used at a concentration of 15 μM. 3-AmPR, 3-AAD, and 3-AADP were each used at a concentration of 1.5 mM and were added to NR (1:100) in BHI growth medium. +, normal growth; −, no growth.

The other strains tested, *H. influenzae* Δ*ompP2*::*cat*, REI1012 (Δ*hel*), REI1010 (*nadN*), and GK04 (Δ*hel nadN*), were resistant to the inhibitors 3-AADP and 3-AAD (NR–3-AADP and NR–3-AAD each at a ratio of 1:100) but were sensitive to 3-AmPR (NR–3-AmPR at a ratio of 1:100) (Table 3). For example, the *ompP2* mutant had a decrease in the V_{max} for the uptake of NAD and NMN but not for the uptake of NR (1). It seems plausible that the facilitated diffusion of 3-AADP and 3-AAD in an *ompP2* mutant is also decreased and, therefore, that this mutant is resistant to 3-AADP and 3-AAD; however, the entry of 3-AmPR is not affected. *nadN* and *hel* mutants lacking NAD nucleotidase and nucleotide phosphatase activities in the periplasm (16), and therefore, 3-AAD(P) is not further hydrolyzed to 3-AmPR. Hence, *nadN* and *hel* mutants are resistant to 3-AAD(P) but sensitive to 3-AmpR (Table 3). To summarize, in the wild-type strain, 3-AAD(P) crosses the outer membrane via OmpP2 and becomes a substrate for NadN and *e*(P4). This leads to the product 3-AmPR, which can be transported further into the cell by PnuC, and a less active NR uptake pathway, which has not yet been identified (15). Therefore, these mutant analyses indicate that 3-AADP, 3-AAD, and 3-AmPR follow the same uptake pathway as NADP, NAD, and NR (1, 15, 19, 33).

To investigate the inhibitory effects of 3-AmPR derivatives on other members of the family *Pasteurellaceae*, we examined the growth of *P. multocida* A3 and *A. actinomycetemcomitans* (Table 3). However, after ON growth in BHI medium supplemented with NR and 3-AADP, 3-AAD, or 3-AmPR, each at a 1:100 ratio, we could not observe any growth inhibition, indicating that at least under these conditions 3-AmPR does not seem to act as an inhibitor. To investigate NAD utilization, [^{14}C]NR uptake was measured in these bacterial strains. No differences in uptake compared with that of *H. influenzae* were found (data not shown). Therefore, we can indeed show that NR uptake is present in these organisms but that 3-AmPR is not an uptake inhibitor. What else could be responsible for such a phenotype? One possibility might be that the NadV homologs in *A. actinomycetemcomitans* and *P. multocida* possess higher levels of activity. It is relevant that the *nadV* that we cloned into *H. influenzae* (15) is derived from *H. ducreyi* and is more related to the *nadV* derived from *Shewanella* and *Mycoplasma* than to that derived from *A. actinomycetemcomitans* and *P. multocida* (27). A putatively more active form of NadV in these two bacterial species may lead to elevated internal concentrations of NMN derived from Nam, and cells would thereby be less sensitive to 3-AmPR. Other possibilities include different specificities of PnuC or NadR, which might have result in a lower affinity for 3-AmPR. Taken together, the results of these experiments indicate that 3-AmPR is effective against *H. influenzae*, but evaluation of its potential to target isolates of the family *Pasteurellaceae* would certainly require more investigations on the NAD utilization of bacterial species of this family.

TABLE 4. Mutant analysis of *nadR* conferring 3-AmPR resistance in *H. influenzae*

Mutations	Amino acid position/motif	5′–3′[a]
Amino acid exchange	161	CAT (His)→CCT (Pro)
	193	GAT (Asp)→TAT (Tyr)
	214	TGG (Trp)→TGT (Cys)
	301/Walker B	GCA (Ala)→GAA (Glu)
	307	TTC (Phe)→GTC (Val)
	322	CAT (His)→CTT (Leu)
Frameshift mutation (insertion)	234/P loop	GGA→GG**G** **G**A
	234/P loop	GGA→GG**G** A
	372	GAT→G**TG TTT AG**A T
Frameshift mutation (duplication)	394	AAA→A**TC TTG ATC GCT ATA ACC AAG TTA** AA
Frameshift mutation (deletion)	240/P loop	AGC→GC
	283/284	GCG CTT→GCT T

[a] Inserted nucleotides are marked in boldface.

Mutant analysis of 3-AmPR-resistant *H. influenzae* isolates. To test the ability of *H. influenzae* to acquire 3-AmPR resistance mutations, a growth selection assay was performed to screen for survivors on 3-AmPR-supplemented growth medium. As a test strain we used SE01 (*nadV*$^+$), which has the ability to utilize both NR and Nam but which is sensitive to the presence of AAD or 3-AmPR (Table 3). We used that strain because it allows us to obtain mutants for NR uptake and NMN resynthesis without interfering with essential growth functions, since NadV scavenges Nam and produces NMN in a PnuC- and an NadR-independent way. Among the mutants isolated, we focused on those mutations which could affect either transport (PnuC) or the biosynthesis of NAD (NadR). We identified mutations that mapped to the *nadR* gene (Table 4) but not to *pnuC* and a few mutants with no mutations in either allele, indicating other origins of 3-AmPR resistance. Recently, NadR was characterized in vitro and shown to exhibit a C′-terminal NR kinase and a N′-terminal adenylyltransferase domain (20, 37). The mutations that we found almost all clustered in the C′-terminal half of NadR, and we found some of them in the P loop or Walker B region (Table 4), according to protein structural and sequence identification (20, 37). These mutations could indicate that while growth is possible by utilizing Nam and converting it into NMN via NadV (27), the synthesis of 3-AAD is blocked most likely because phosphorylation of 3-AmPR via the mutated NR kinase domain of NadR is insufficient to produce the 3-AAD precursor, AMN. We do not know why we could not isolate *pnuC* mutants in this screen, even knowing that Δ*pnuC* confers 3-AmPR resistance (Fig. 5; Table 3). It might be that mutations in PnuC occur at a lower frequency and that a higher number of resistant mutants would be required to obtain those.

To further test whether NadR activity is inhibited by 3-AAD or 3-AmPR or whether it utilizes 3-AmPR to synthesize 3-AAD, we tested a recombinant His-tagged NadR protein. Investigation of NAD biosynthesis in an in vitro assay with [^{14}C]NR with 3-AmPR or 3-AAD at a ratio of 1:10 or 1:25 showed no difference in the synthesis of [^{14}C]NAD observed (data not shown). Therefore, we can confirm in vitro, as already shown for *H. influenzae* cell extracts (5), that the growth-inhibitory action of 3-AAD is not due to an inhibition of NAD biosynthesis. Furthermore, we tested the in vitro ability of His-tagged NadR to synthesize 3-AAD derived from 3-AmPR and ATP and found that NadR is indeed able to produce 3-AAD (Fig. 6A and B). Therefore, we conclude that under in vivo conditions the organisms produce 3-AAD derived from 3-AmPR, most likely via NadR, and that 3-AAD then competes for NAD in the corresponding NAD^+ and $NADH + H^+$ redox systems.

Interestingly, it was only because of the finding of the NadR-associated NR kinase and NMN adenylyltransferase activities of *E. coli* and *H. influenzae* (20, 32, 37) which led to the identification of NR as an unanticipated NAD^+ precursor in yeast (3). Therefore, it is highly likely that NR kinase in humans seems to be responsible for nucleotide analogue-based prodrug conversion. In that sense, activation of nucleotide antitumor prodrugs, such as benzamide riboside, tiazofurin, and selenazofurin, follows a route similar to that shown here for 3-AmPR. For example, the prodrug benzamide riboside is applied to cancer cells and taken up by an unknown mechanism, and then when it is inside the cell it is used as a substrate to synthesize benzamide adenine dinucleotide (BAD) by the action of a NMN adenylyltransferase. BAD then acts as a noncompetitive inhibitor of IMP dehydrogenase, which leads to the depletion of guanylates (GTP and dGTP) and, subsequently, to apoptosis (10, 47). BAD also inhibits poly(ADP-ribose) polymerase, which influences p53 expression, which then leads to apoptosis (46). So far the target of 3-AAD-mediated growth inhibition in *H. influenzae* is unknown. From previous studies we know that, for example, under aerobic growth conditions NAD^+-dependent pyruvate dehydrogenase knockout mutations cause growth arrest, which is associated with virulence deficiency (14). However, as shown here, 3-AAD also acts as an inhibitor under anaerobic growth conditions (Fig. 5, bars 1a), indicating that 3-AAD inhibition might instead target anabolism, for example, nucleotide synthesis (see above) and then metabolism.

Conclusions. This study focused on the 3-AAD utilization pathway of *H. influenzae* in which the major NR permease, PnuC, is involved. We report a detailed topology analysis of

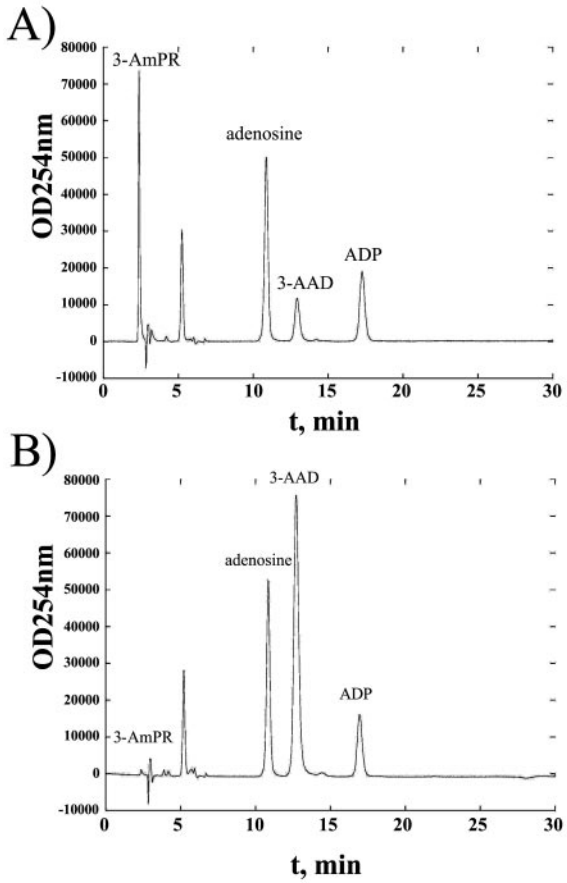

FIG. 6. HPLC analysis of His-tagged NadR synthesis of 3-AAD in vitro. The 3-AAD reaction is shown as a control consisting of the reaction mixture described in Material and Methods without His-tagged NadR (A) and the same reaction with His-tagged NadR (0.05 mg/ml) (B). The appearance of 3-AAD and the disappearance of 3-AmPR were monitored. The peaks identified in the graph were verified by UV spectral analysis (data not shown). The *x* axis corresponds to the retention time (t), and the *y* axis corresponds to UV absorption at 254 nm.

PnuC, its membrane localization, and a functional comparison of *H. influenzae* PnuC with *E. coli* PnuC, in which we show that NR serves as the final substrate for PnuC-based uptake. Considering the distant relationship of the PnuC proteins of *H. influenzae* and *E. coli*, we claim that other annotated PnuC proteins represent NR-specific permeases. Following previous inhibitor studies (11) with 3-AmPR and *H. influenzae*, we demonstrated that 3-AAD is converted to 3-AmPR for uptake by the NAD to NR processing and utilization pathway. In in vitro studies, we show that resynthesis from 3-AmPR to 3-AAD can be achieved by NadR. For confirmation we identified various *nadR* mutants, selected for by growth in the presence of 3-AmPR in an *nadV*$^+$ background. In addition, we showed that wild-type *H. influenzae* and a Δ*pnuC* mutant are sensitive to 3-AmPR. However, if *nadV*$^+$ is present, then Δ*pnuC* mutants are resistant to 3-AmPR, indicating that the bulk entry of 3-AmPR occurs via PnuC. This phenotype could be explained by assuming that the amount of NMN produced via NadV is large enough to allow sufficient NAD synthesis for growth if less 3-AmPR can enter the cell, e.g., because of a Δ*pnuC* mutation. No inhibitory effect of 3-AmPR against other isolates of the family *Pasteurellaceae* could be found, e.g., *P. multocida* and *A. actinomycetemcomitans*. It could be that the inherited ability for Nam utilization might be much more efficient in these organisms than in the *nadV*$^+$ *H. influenzae* strain constructed. Under these circumstances, elevated levels of production of NMN derived from Nam would compensate for the higher level of competitive 3-AmPR influx via PnuC. This may indicate that during evolution Nam utilization may have had preference over NAD utilization for these organisms. Further investigations are needed to characterize the molecular mechanism of NR and Nam utilization in *Pasteurella* and *Actinobacillus* spp.

ACKNOWLEDGMENTS

We thank M. Herbert for suggestions and critical reading of the manuscript. We are grateful to M. K. Bhattacharjee and L. Weiler for strains *A. actinomycetemcomitans* CU4000N and *P. multocida* A3. We thank M. Ehrmann for plasmid pSWFII.

This work was supported by "Deutsche Forschungsgemeinschaft" grant Re1561/1, Sonderforschungsbereich 630, and the "Fonds der Chemischen Industrie."

REFERENCES

1. **Andersen, C., E. Maier, G. Kemmer, J. Blass, A. K. Hilpert, R. Benz, and J. Reidl.** 2003. Porin OmpP2 of *Haemophilus influenzae* shows substrate specificity towards nicotinamide-derived nucleotide substrates. J. Biol. Chem. **278:**24269–24276.
2. **Barcak, G. J., M. S. Chandler, R. J. Redfield, and J. F. Tomb.** 1991. Genetic systems in *Haemophilus influenzae*. Methods Enzymol. **204:**321–342.
3. **Bieganowski, P., and C. Brenner.** 2004. Discoveries of nicotinamide riboside as a nutrient and conserved NRK genes establish a Preiss-Handler independent route to NAD$^+$ in fungi and humans. Cell **117:**495–502.
4. **Brentjens, R. J., M. Ketterer, M. A. Apicella, and S. M. Spinola.** 1996. Fine tangled pili expressed by *Haemophilus ducreyi* are a novel class of pili. J. Bacteriol. **178:**808–816.
5. **Denicola-Seoane, A., and B. M. Anderson.** 1990. Studies of NAD kinase and NMN:ATP adenylyltransferase in *Haemophilus influenzae*. J. Gen. Microbiol. **136:**425–430.
6. **Evans, N. M., D. D. Smith, and A. J. Wicken.** 1974. Hemin and nicotinamide adenine dinucleotide requirements of *Haemophilus influenzae*. J. Med. Microbiol. **7:**359–365.
7. **Fine, D. H., D. Furgang, J. Kaplan, J. Charlesworth, and D. H. Figurski.** 1999. Tenacious adhesion of *Actinobacillus actinomycetemcomitans* strain CU1000 to salivary-coated hydroxyapatite. Arch. Oral Biol. **44:**1063–1076.
8. **Fisher, T. L., S. V. Vercellotti, and B. M. Anderson.** 1973. Interactions of 3-aminopyridine adenine dinucleotide with dehydrogenases. J. Biol. Chem. **248:**4293–4299.
9. **Fleischmann, R. D., M. D. Adams, O. White, R. A. Clayton, E. F. Kirkness, A. R. Kerlavage, C. J. Bult, J. F. Tomb, B. A. Dougherty, J. M. Merrick, K. McKenney, G. Sutton, W. FitzHugh, C. Fields, J. D. Gocayne, J. Scott, R. Shirley, L. I. Liu, A. Glodek, J. M. Kelley, J. F. Weidman, C. A. Phillips, T. Spriggs, E. Hedblom, M. D. Cotton, T. R. Utterback, M. C. Hanna, D. T. Nguyen, D. M. Saudek, R. C. Brandon, L. D. Fine, J. L. Frichman, J. L. Fuhrmann, N. S. M. Geoghagen, C. L. Gnehm, L. A. McDonald, K. V. Small, C. M. Fraser, H. O. Smith, and J. C. Venter.** 1995. Whole-genome random sequencing and assembly of *Haemophilus influenzae* Rd. Science **269:**496–512.
10. **Franchetti, P., and M. Grifantini.** 1999. Nucleoside and non-nucleoside IMP dehydrogenase inhibitors as antitumor and antiviral agents. Curr. Med. Chem. **6:**599–614.
11. **Godek, C. P., and M. H. Cynamon.** 1990. In vitro evaluation of nicotinamide riboside analogs against *Haemophilus influenzae*. Antimicrob. Agents Chemother. **34:**1473–1479.
12. **Green, B. A., J. E. Farley, T. Quinn-Dey, R. A. Deich, and G. W. Zlotnick.** 1991. The *e* (P4) outer membrane protein of *Haemophilus influenzae*: biologic activity of anti-*e* serum and cloning and sequencing of the structural gene. Infect. Immun. **59:**3191–3198.
13. **Grimberg, J., S. Maguire, and L. Belluscio.** 1989. A simple method for the preparation of plasmid and chromosomal *E. coli* DNA. Nucleic Acids Res. **17:**8893.
14. **Herbert, M. A., A. Kraiβ, A.-K. Hilpert, and J. Reidl.** 2003. Aerobic growth deficient *Haemophilus influenzae* mutants are non-virulent in the rat model: implications on metabolism. J. Int. Med. Microbiol. **293:**145–152.

15. **Herbert, M. A., E. Sauer, G. Smethurst, A. Kraiβ, A.-K. Hilpert, and J. Reidl.** 2003. Identification and characterization of nicotinamide-ribosyl uptake mutants in *Haemophilus influenzae*. Infect. Immun. **71:**5398–5401.
16. **Kadner, R. J.** 1996. Cytoplasmic membrane, p. 58–87. *In* F. C. Neidhardt, R. Curtis III, J. L. Ingraham, E. C. C. Lin, K. B. Low, B. Magasanik, W. S. Reznikoff, M. Schaechter, and H. E. Umbarger (ed.), *Escherichia coli* and *Salmonella typhimurium*: cellular and molecular biology, vol. 1, 2nd ed. American Society for Microbiology, Washington, D.C.
17. **Kahn, D. W., and B. M. Anderson.** 1986. Characterization of *Haemophilus influenzae* nucleotide pyrophosphatase. J. Biol. Chem. **261:**6016–6025.
18. **Kasarov, L. B., and A. G. Moat.** 1972. Convenient method for enzymatic synthesis of ^{14}C-nicotinamide riboside. Anal. Biochem. **46:**181–186.
19. **Kemmer, G., T. Reilly, J. Schmidt-Brauns, G. W. Zlotnik, B. A. Green, M. J. Fiske, M. Herbert, A. Kraiβ, S. Schlör, A. Smith, and J. Reidl.** 2001. NadN and *e*(P4) are essential for the utilization of NAD and NMN but not NR in *Haemophilus influenzae*. J. Bacteriol. **183:**3974–3981.
20. **Kurnasov, O. V., B. M. Polanuyer, S. Ananta, R. Sloutsky, A. Tam, S. Y. Gerdes, and A. L. Osterman.** 2002. Ribosylnicotinamide kinase domain of NadR protein: identification and implications in NAD biosynthesis. J. Bacteriol. **184:**6906–6917.
21. **Laemmli, U. K.** 1970. Cleavage of structural proteins during the assembly of the head of bacteriophage T4. Nature **227:**680–685.
22. **Lee, C., P. Li, H. Inouye, E. R. Brickman, and J. Beckwith.** 1989. Genetic studies on the inability of β-galactosidase to be translocated across the *Escherichia coli* cytoplasmic membrane. J. Bacteriol. **171:**4609–4616.
23. **Maniatis, T., E. F. Fritsch, and J. Sambrook.** 1989. Molecular cloning: a laboratory manual, 2nd ed. Cold Spring Harbor Laboratory Press, Cold Spring Harbor, N.Y.
24. **Manoil, C.** 1991. Analysis of membrane protein topology using alkaline phosphatase and β-galactosidase gene fusion. Methods Cell Biol. **34:**61–75.
25. **Manoil, C.** 1990. Analysis of protein localization by use of gene fusions with complementary properties. J. Bacteriol. **172:**1035–1042.
26. **Manoil, C., and J. Beckwith.** 1985. Tn*phoA*: a transposon probe for protein export signals. Proc. Natl. Acad. Sci. USA **82:**8129–8133.
27. **Martin, P. R., R. J. Shea, and M. H. Mulks.** 2001. Identification of a plasmid-encoded gene from *Haemophilus ducreyi* which confers NAD independence. J. Bacteriol. **183:**1168–1174.
28. **Mazur, A., J. E. Krol, M. Marczak, and A. Skorupska.** 2003. Membrane topology of PssT, the transmembrane protein component of the type I exopolysaccharide transport system in *Rhizobium leguminosarum* bv. trifolii strain TA1. J. Bacteriol. **185:**2503–2511.
29. **Miller, J. H.** 1972. Experiments in molecular genetics. Cold Spring Harbor Laboratory, Cold Spring Harbor, N.Y.
30. **Niven, D. F., and T. O'Reilly.** 1990. Significance of V-factor dependency in the taxonomy of *Haemophilus* species and related organisms. Int. J. Syst. Bacteriol. **40:**1–4.
31. **O'Reilly, T., and D. F. Niven.** 1986. Pyridine nucleotide metabolism by extract derived from *Haemophilus parasuis* and *H. pleuropneumoniae*. Can. J. Microbiol. **32:**733–737.
32. **Raffaelli, N., P. L. Lorenzi, M. Emanuelli, A. Amici, S. Ruggieri, and G. Magni.** 1999. The *Escherichia coli* NadR regulator is endowed with nicotinamide mononucleotide adenylyltransferase activity. J. Bacteriol. **181:**5509–5511.
33. **Reidl, J., S. Schloer, A. Kraiss, J. Schmidt-Brauns, G. Kemmer, and E. Soleva.** 2000. NADP and NAD utilization in *Haemophilus influenzae*. Mol. Microbiol. **35:**1573–1581.
34. **Rose, R. E.** 1988. The nucleotide sequence of pACYC184. Nucleic Acids Res. **16:**355.
35. **Schmidt-Brauns, J., M. Herbert, G. Kemmer, A. Kraiβ, S. Schlör, and J. Reidl.** 2001. Is a NAD-pyrophosphatase activity needed by *Haemophilus influenzae* type b for multiplication in the blood stream? Int. J. Med. Microbiol. **291:**219–225.
36. **Shifrine, M., and E. L. Biberstein.** 1960. A growth factor for *Haemophilus* species secreted by a pseudomonad. Nature **187:**623.
37. **Singh, S. K., O. V. Kurnasov, B. Chen, H. Robinson, N. V. Grishin, A. L. Osterman, and H. Zhang.** 2002. Crystal structure of *Haemophilus influenzae* NadR protein: a bifunctional enzyme endowed with NMN adenylyltransferase and ribosylnicotinamide kinase activities. J. Biol. Chem. **277:**33291–33299.
38. **Sonnhammer, E. L., G. von Heijne, and A. Krogh.** 1998. A hidden Markov model for predicting transmembrane helices in protein sequences. Proc. Int. Conf. Intell. Syst. Mol. Biol. **6:**175–182.
39. **Spector, M. P., J. M. Hill, E. A. Holley, and J. W. Foster.** 1985. Genetic characterization of pyridine nucleotide uptake mutants of *Salmonella typhimurium*. J. Gen. Microbiol. **131:**1313–1322.
40. **Taylor, L. A., and R. E. Rose.** 1988. A correction in the nucleotide sequence of the Tn*903* kanamycin resistance determinant in pUC4K. Nucleic Acids Res. **16:**7762.
41. **Towbin, H., T. Staehlin, and J. Gordon.** 1979. Electrophoretic transfer of proteins. Proc. Natl. Acad. Sci. USA **76:**4350–4354.
42. **Vella, P. P., and W. R. Ellis.** 1992. *Haemophilus* b conjugate vaccine, p. 1–20. *In* R. W. Ellis (ed.), Vaccines. Butterworth-Heinemann, Stoneham, United Kingdom.
43. **Windsor, H. M., R. C. Gromkova, and H. J. Koornhof.** 1993. Growth characteristics of V factor-independent transformants of *Haemophilus influenzae*. Int. J. Syst. Bacteriol. **43:**799–804.
44. **Windsor, H. M., R. C. Gromkova, and H. J. Koornhof.** 1991. Plasmid-mediated NAD independence in *Haemophilus parainfluenzae*. J. Gen. Microbiol. **137:**2415–2421.
45. **Windsor, H. M., R. C. Gromkova, and H. J. Koornhof.** 1993. Transformation of V-factor independence fom *Haemophilus ducreyi* to *Haemophilus influenzae* and *Haemophilus parainfluenzae*. Med. Microbiol. Lett. **2:**159–167.
46. **Yalowitz, J. A., and H. N. Jayaram.** 2002. Modulation of cytotoxicity of benzamide riboside by expression of NMN adenylyltransferase. Curr. Med. Chem. **9:**748–758.
47. **Yalowitz, J. A., and H. N. Jayaram.** 2000. Molecular targets of guanine nucleotides in differentiation, proliferation and apoptosis. Anticancer Res. **20:**2329–2338.
48. **Yoon, H., and B. M. Anderson.** 1989. Site-directed inhibition of *Haemophilus influenzae* malate dehydrogenase. J. Gen. Microbiol. **135:**245–250.
49. **Yoon, H., C. D. Anderson, and B. M. Anderson.** 1989. Kinetic studies of *Haemophilus influenzae* 6-phosphogluconate dehydrogenase. Biochem. Biophys. Acta **994:**75–80.
50. **Zhu, N., B. M. Olivera, and J. R. Roth.** 1991. Activity of the nicotinamide mononucleotide transporter system is regulated in *Salmonella typhimurium*. J. Bacteriol. **173:**1311–1320.
51. **Zhu, N., M. Olivera, and J. R. Roth.** 1989. Genetic characterization of the *pnuC* gene, which encodes a component of the nicotinamide mononucleotide transport system in *Salmonella typhimurium*. J. Bacteriol. **171:**4402–4409.